

THE BEAM DYNAMICS UPDATES OF THE FERMILAB PIP-II 800 MeV SUPERCONDUCTING LINAC*

A. Saini[†], V. Yakovlev, E. Pozdeyev, Fermilab, Batavia, USA

Abstract

The Proton Improvement Plan (PIP) -II is a high intensity proton facility being developed to support a neutrino program over the next two decades at Fermilab. At its core is the design and construction of a Continuous Wave (CW) compatible superconducting radio frequency (SRF) linear accelerator that would accelerate an average beam current of 2 mA up to 800 MeV. This paper presents recent updates in the beam dynamics leading to a reliable and robust linac design and simplifying the cryomodule assembly.

INTRODUCTION

Fermilab is planning to perform a systematic upgrade of its existing accelerator complex to support a world leading neutrino program and rich variety of high intensity frontier particle physics experiments. An extensive roadmap named, 'Proton Improvement Plan (PIP)' is established to implement these upgrades. The second stage of the proton improvement plan (PIP-II) is devised to enable the Fermilab accelerator complex to deliver a beam power in excess of mega-watt (MW) on target at the initiation of Long Baseline Neutrino Facility [1]. This in turn, requires construction of a new Continuous Wave (CW)-compatible SRF linac. It is designed to deliver H⁺ ions beam with a final kinetic energy of 800 MeV and an average current of 2 mA endowed with a special and flexible time structure to satisfy diverse experimental needs. A detailed description of the PIP-II linac was presented elsewhere [2].

SRF LINAC ARCHITECTURE

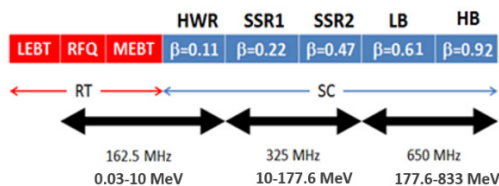


Figure 1: Acceleration scheme in the PIP-II linac. Red-coloured sections operate at room temperature while blue-coloured sections operate at 2K.

A schematic of the linac's architecture is shown in Fig. 1. It is composed of a warm front-end and an SRF accelerating section. The warm front-end consists of an ion source, a Low Energy Beam Transport (LEBT) line, an RFQ and, a Medium Energy Beam Transport line. Most of the beam manipulations happen in this part of the linac. The beam acceleration occurs mainly in the SRF linac that utilizes

five families of superconducting cavities to accelerate the H⁺ ion beam from kinetic energy of 2.1 MeV to 800 MeV. Based on these families, the SRF linac is segmented into five sections i.e. Half Wave Resonator (HWR), Single Spoke Resonator (SSR) 1 & 2, Low Beta (LB) and High Beta (HB). Each of them is represented in Fig. 1 using optimal beta of respective cavities except LB and HB sections which are shown using geometrical betas. Number of cryomodules (CM) and their configurations in each section are summarized in Table 1. Note that superconducting solenoids are used in HWR, SSR1 and SSR2 sections while warm quadrupole doublets are utilized in LB and HB sections.

Table 1: Numbers of Elements and Energy Range in Each Section of the PIP-II SRF LINAC

Section	CM	Cav/Mag per CM	Energy (MeV)
HWR	1	8/8	2.1-10
SSR1	2	8/4	10-32
SSR2	7	5/3	32-177
LB	9	4/1*	177-516
HB	4	6/1*	516-833

*one warm quadrupole doublet located between cryomodules in LB and HB sections

Progress Towards Baseline Design

In course of evolution from a conceptual design to the baseline design, the PIP-II linac accommodates a few changes that have been made to address technical risks, cost minimization and operational reliability. Some of the major configurational changes are summarized below:

- The LB CM is elongated to include an additional cavity. In the baseline design, LB section is made of nine CMs and each of them houses a total of four 5-cell elliptical cavities. Note that, LB section in the conceptual design included a total of eleven CMs whereas each CM was composed of three cavities. Figure 2 showed a comparison in focusing periods in three and four cavity CMs. An additional cavity results in an increase in transverse focusing period. Consequently, resulting increase in transverse beta functions were managed by increasing quadrupole strengths. Furthermore, the linac's total length remained unchanged because of a smaller number of magnets. A total increase of three cavities in LB section will enhance operational reliability of the linac by providing not only an energy margin in case of a fault scenario but also a higher transition energy at HB650 entrance. This in turn leads to a gain in performance of the HB650 cavities.

* Work supported by Fermi Research Alliance, LLC under contract no. DE-AC02-07CH11359 with the DOE, USA

[†]asaini@fnal.gov

- A dedicated space of 250 mm is allocated for collimators between SSRs CMs. This arrangement will assist to reduce potential beam loss in cryogenic environment and thereby minimize un-controlled beam loss in the linac.
- As engineering design of components get matured, their space allocation requirements were revisited. There is an increase of 75 mm between neighbouring cavities in SSR1 CM. Also, space allocation for the quadrupole doublet in SRF linac is increased about 250 mm.

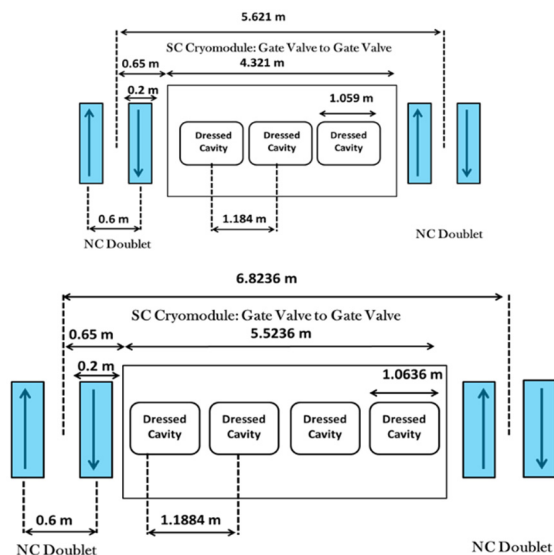


Figure 2: Focusing period in LB650 section for (top) 3-cavity and (bottom) 4-cavity cryomodule. Note that, upward and downward arrows depict vertical focusing and defocusing quadrupole respectively.

RECENT DEVELOPMENT AT PIP2IT

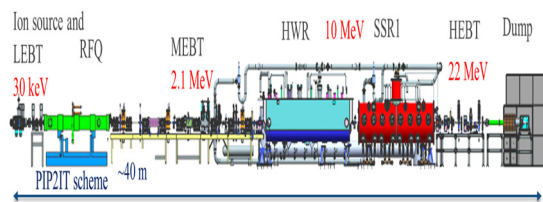


Figure 3: A schematic of the PIP2IT facility.

It is well known that most of the technological and beam-physics risks and issues in an ion linac are associated with its front-end. To address and mitigate these risks, an accelerator test facility named PIP-II Injector Test (PIP2IT) is under construction at Fermilab that would demonstrate technologies and design choices made for the PIP-II linac. Figure 3 showed a layout of the PIP2IT facility. A detail description had been provided elsewhere [3]. In present, a complete warm-front end had been installed and commissioned [4] at the PIP2IT. A variety of the beam optics measurements [5-6] were performed to characterize the beam profiles, RMS emittances, beam-energy, chopping scheme etc. Initial Twiss functions were reconstructed at

exit of the RFQ. These Twiss functions are utilized to design baseline optics of the PIP-II linac. The SRF section in the PIP2IT, made of a cryomodule of each HWR and SSR1. Figure 4 showed a string assembly of the SSR1 CM. Note that, both cryomodules are in their final stage of constructions and scheduled to commission by early spring in 2020. A successful commissioning of the complete PIP2IT will eliminate most of the operational risks and therefore, attest a major milestone toward realization of the PIP-II SRF linac.

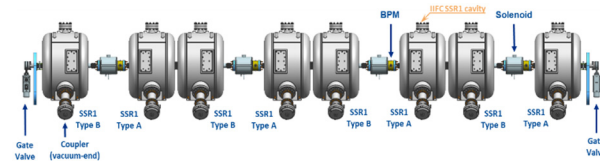


Figure 4: A string assembly of SSR1 cryomodule that includes four superconducting solenoids and eight SSR1 resonators arranged in a period of Cavity-Solenoid-Cavity. A detailed description has been presented elsewhere [7].

BASELINE OPTICS

A robust optics has been designed using principles and considerations that had been discussed elsewhere [8]. To account an uncertainty in longitudinal emittance, the baseline optics has been developed with a 20% higher longitudinal emittance at the exit of the RFQ in comparison to a conceptual design optics. Accelerating voltages and phases in cavities were optimized to obtain a rapid beam acceleration as well as a smooth adiabatic beam envelope. Figure 5 showed voltage amplitude settings in cavities for the baseline optics. It can be deduced from Fig. 5 that a few first cavities in each section are not operating at their maximum available voltage. This is done to perform a beam-matching between sections that accounts variation in focusing periods in each section.

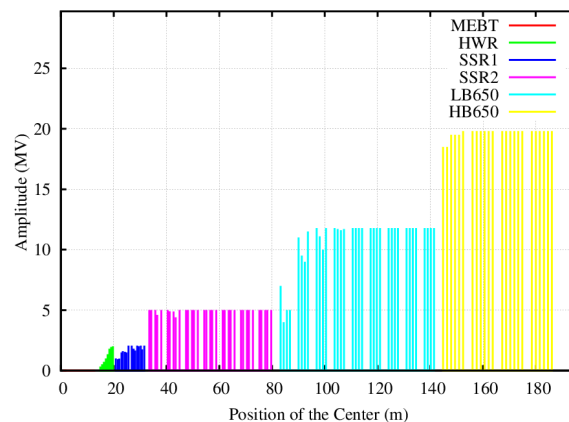


Figure 5: Voltage amplitude settings in cavities along the linac for the baseline optics.

Figure 6 showed axial fields in solenoids and integral fields in quadrupoles. Solenoids are designed to operate at maximum axial fields of 6T whereas design specification for the integral magnetic field in quadrupoles (in SRF linac) is 3T. Note that same family of quadrupoles is used in both LB and HB sections.

Content from this work may be used under the terms of the CC BY 3.0 licence (© 2019). Any distribution of this work must maintain attribution to the author(s), title of the work, publisher, and DOI.

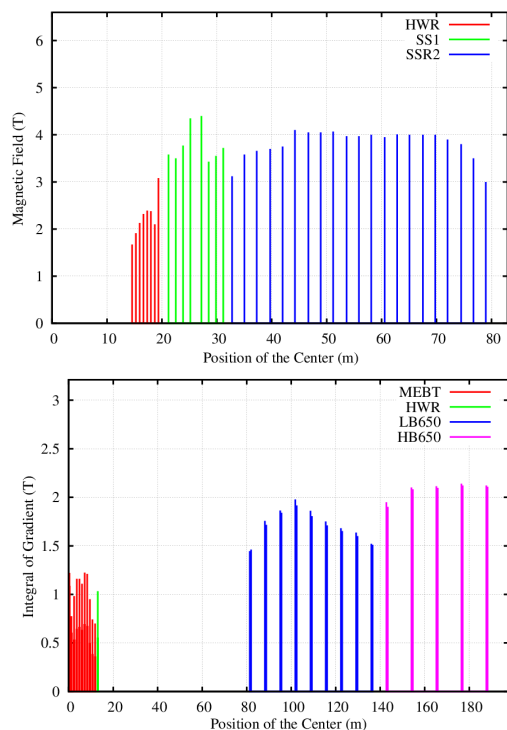


Figure 6: Axial fields (top) and integral fields (bottom) settings in solenoids and quadrupoles respectively for the baseline optics.

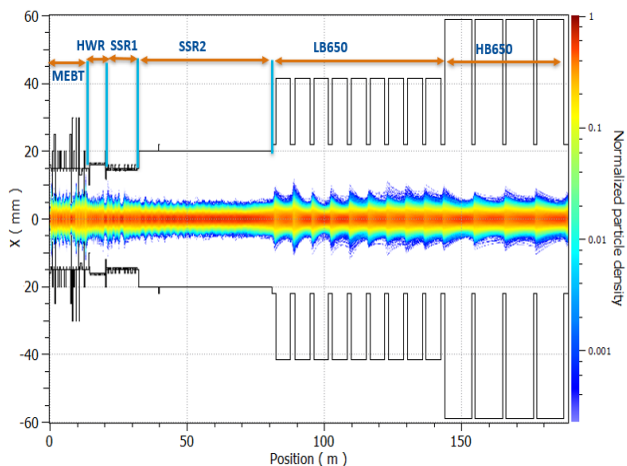


Figure 7: Beam density projection in horizontal plane along with aperture limitation through the RFQ exit to the linac end.

A multiparticle simulation using TRACEWIN [9] was performed for a nominal beam current of 5mA. Figure 7 showed horizontal particle density evolution along the linac for a 6D Gaussian distribution of 100k macro-particles truncated at 6σ . Note that, σ is RMS beam size. A similar beam profile was obtained in the vertical plane. It can also be noted from Fig. 7 that aperture constraints are more stringent at low energy part of the linac especially in HWR and SSR1 sections. In rest of the linac, apertures are sufficiently large to transmit even 10 to 12σ beam. There was no beam loss observed in SRF linac for the nominal optics.

A small fraction of beam was intercepted at scrapers positioned in the MEBT to limit the maximum action of particles entering to SRF linac.

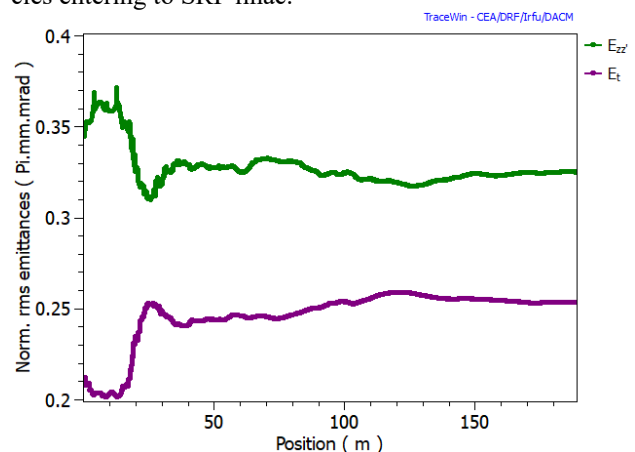


Figure 8: RMS normalized transverse (magenta) and longitudinal (green) emittance along the linac.

Figure 8 depicted RMS normalized emittances evolution along the linac. There is about 21 % growth of transverse emittance whereas longitudinal emittance is reduced by 4 % due to emittance exchange. However, emittance growths are within the design specifications. It can also be noticed from Fig. 8 that most of the emittance exchange occurs at the beginning of the linac where the beam energy is lower and space charge forces are significant. In order to understand optics tolerances against potential errors, longitudinal acceptance of the linac was evaluated. Note that, acceptance determines a largest beam size in given plane that could be transmitted through an accelerator without observing a beam loss. Figure 9 showed that longitudinal acceptance of the PIP-II SRF linac is sufficiently large to enclose a 6σ beam easily.

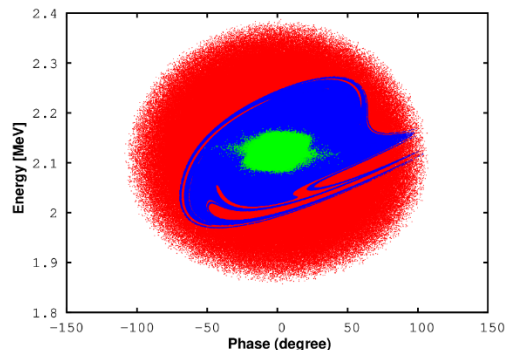


Figure 9: Longitudinal acceptance of the PIP-II SC linac (blue) with 6σ beam (green) at the SRF linac entrance. Initial particle distribution was shown in red.

ACKNOWLEDGEMENTS

Authors takes this opportunity to acknowledge entire PIP-II team and collaborators who are working in harmony for a successful realization of the project.

OUTLOOK

The PIP-II SRF linac design has been advanced to its baseline design. A few changes have been made during this process to mitigate operational risks as well as to facilitate a cost minimization of entire project. One of the most noticeable changes has been a redressing of LB650 section. A complete baseline optics incorporating all necessary changes has been developed for the PIP-II SRF linac. Preliminary beam dynamics studies showed that the linac's basic performance in terms of emittances growth, acceptances, beam envelopes etc remains similar as in earlier variant of the linac. It implies that choices of optics elements and their operating parameters have sufficiently robust to accommodate these changes.

REFERENCES

- [1] The DUNE Collaboration, "CDR Volume 1: The LBNF and DUNE Projects," tech. rep., 2015. <http://1bne2-docdb.fnal.gov/cgi-bin/ShowDocument?docid=10687>.
- [2] PIP-II Conceptual Design Report, 2017, <http://pip2-docdb.fnal.gov/cgi-bin/ShowDocument?docid=113>
- [3] P. Derwent *et al.*, "PIP-II Injector Test: Challenges and Status", in *Proc. 28th Linear Accelerator Conf. (LINAC'16)*, East Lansing, MI, USA, Sep. 2016, pp. 641-645. doi:10.18429/JACoW-LINAC2016-WE1A01

- [4] L. R. Prost *et al.*, "PIP-II Injector Test Warm Front End: Commissioning Update", in *Proc. 9th Int. Particle Accelerator Conf. (IPAC'18)*, Vancouver, Canada, Apr.-May 2018, pp. 2943-2946. doi:10.18429/JACoW-IPAC2018-THYGBF2
- [5] A. Saini, J.-P. Carneiro, B. M. Hanna, L. R. Prost, A. V. Shemyakin, and V. L. Sista, "Beam Optics Measurements in Medium Energy Beam Transport at PIP-II Injector Test Facility", in *Proc. 9th Int. Particle Accelerator Conf. (IPAC'18)*, Vancouver, Canada, Apr.-May 2018, pp. 909-912. doi:10.18429/JACoW-IPAC2018-TUPAF077
- [6] A. V. Shemyakin *et al.*, "Experimental Study of Beam Dynamics in the PIP-II MEBT Prototype", in *Proc. 61st ICFA Advanced Beam Dynamics Workshop on High-Intensity and High-Brightness Hadron Beams (HB'18)*, Daejeon, Korea, Jun. 2018, pp. 54-59. doi:10.18429/JACoW-HB2018-MOP1WB03
- [7] D. Passarelli, D. J. Bice, M. Parise, G. Wu, and S. Berry, "Lessons Learned Assembling the SSR1 Cavities String for PIP-II", presented at the 19th Int. Conf. RF Superconductivity (SRF'19), Dresden, Germany, Jun.-Jul. 2019, paper TUP095.
- [8] A. Saini, "Design Considerations for the Fermilab PIP-II 800 MeV Superconducting Linac", in *Proc. North American Particle Accelerator Conf. (NAPAC'16)*, Chicago, IL, USA, Oct. 2016, pp. 826-829. doi:10.18429/JACoW-NAPAC2016-WEP0A60
- [9] <http://irfu.cea.fr/dacm/logiciels/>